Supplemental Material

LIST OF FIGURES

Distribution of GEBA sites between 1980 and 2015

Fig. S1. Geographic distribution of all the GEBA sites used in this study. The sites used for Common Period I (2001-2015) are shown in Fig. S3.
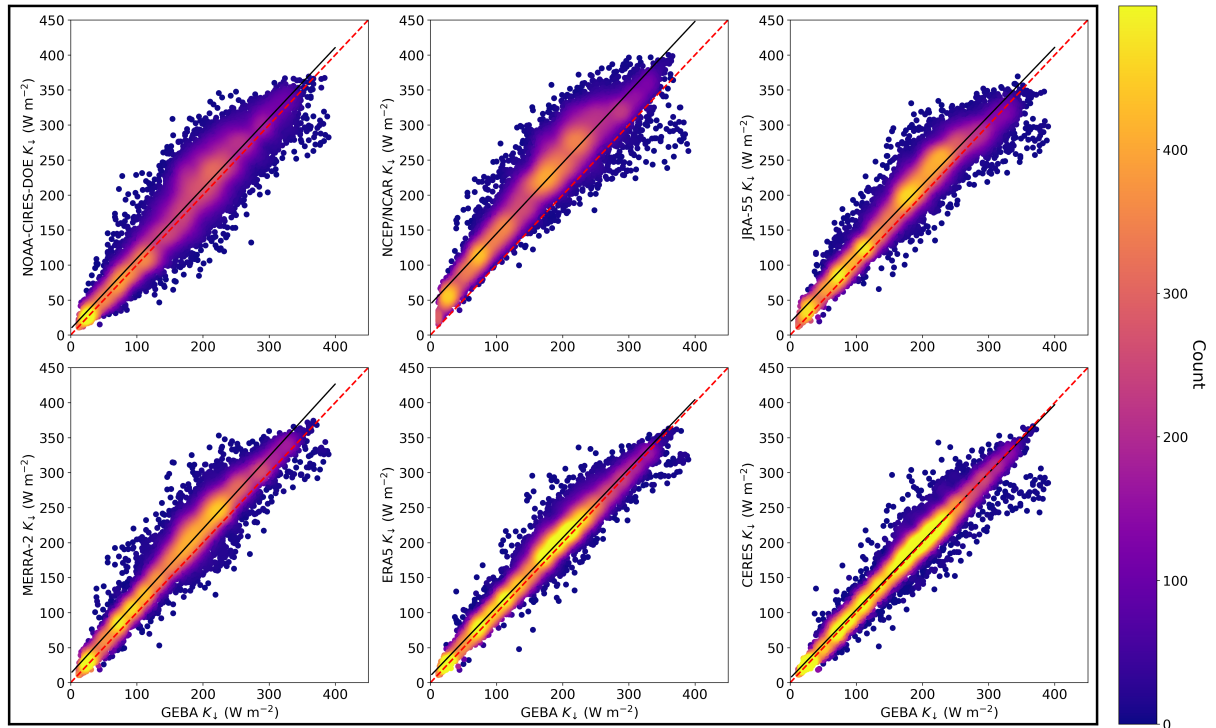
Fig. S2. Evaluations of monthly mean incoming shortwave radiation ($K_\downarrow$) at the surface of gridded reanalysis and CERES products using all common GEBA observations for Common Period I (2001-2015). The red dashed lines represent the 1:1 relationship. Color indicates data density. Statistical summaries of the evaluations are in Table 2 of the main text.
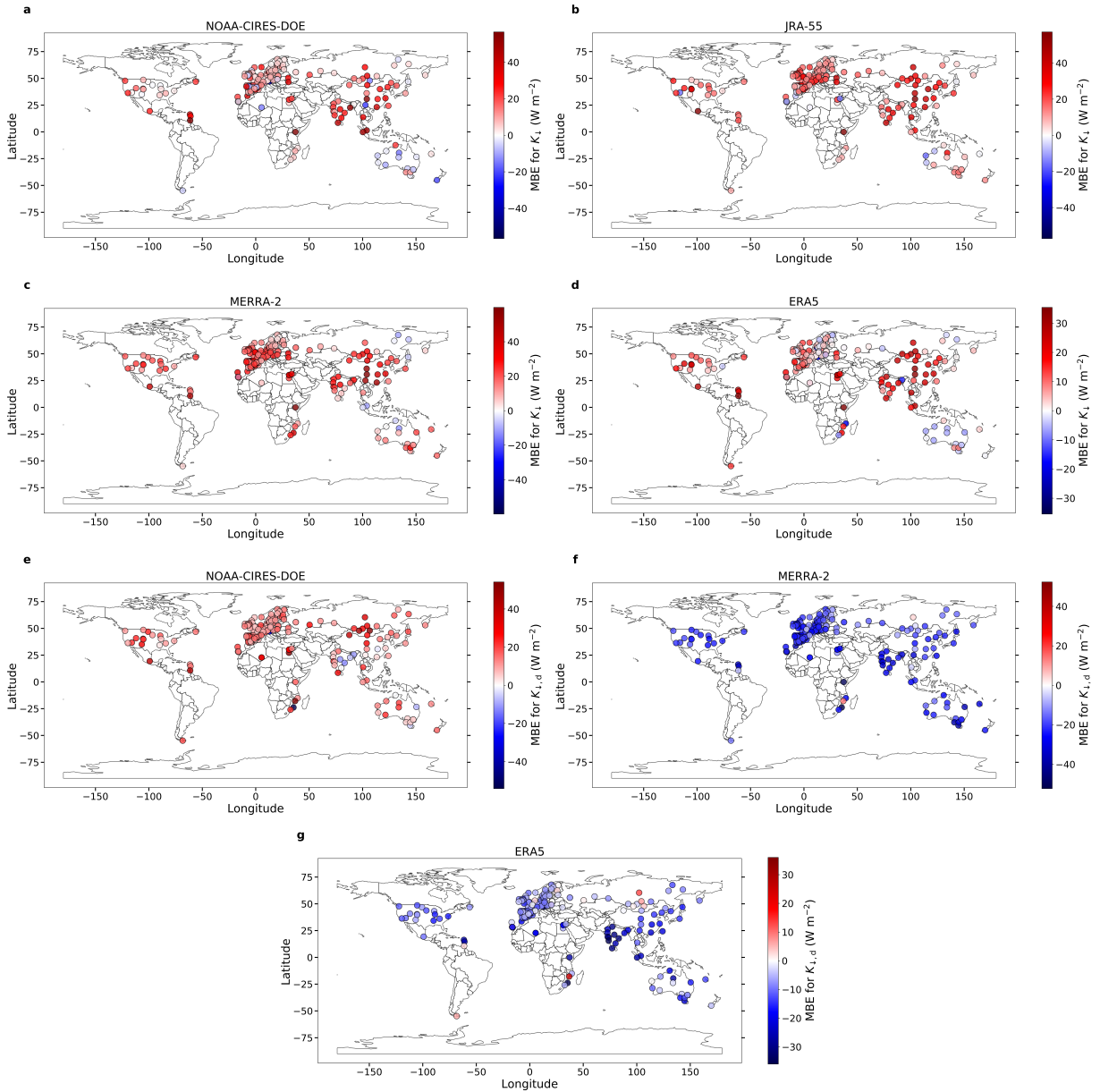
Fig. S3. Site-level mean bias error (MBE) in incoming shortwave radiation ($K_\downarrow$) at the surface for **a** NOAA-CIRES-DOE, **b** JRA-55, **c** MERRA-2, and **d** ERA5 gridded data compared to common GEBA observations for Common Period I (2001-2015). Sub-figures **e**, **f**, and **g** show the corresponding MBE in incoming diffuse radiation ($K_{\downarrow,\mathrm{b}}$) at the surface for NOAA-CIRES-DOE, MERRA-2, and ERA5, respectively.
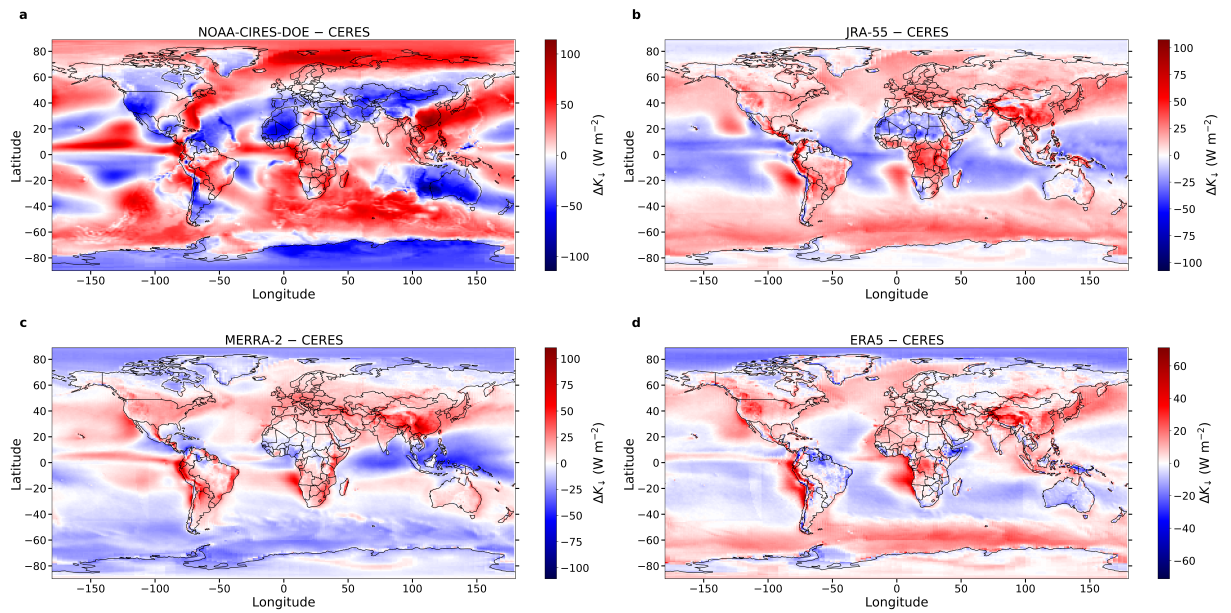
Fig. S4. Grid-wise difference in incoming shortwave radiation ($K_\downarrow$) at surface between CERES data and **a** NOAA-CIRES, **b** JRA-55, **c** MERRA-2, and **d** ERA5, respectively for Common Period I (2001-2015).

5
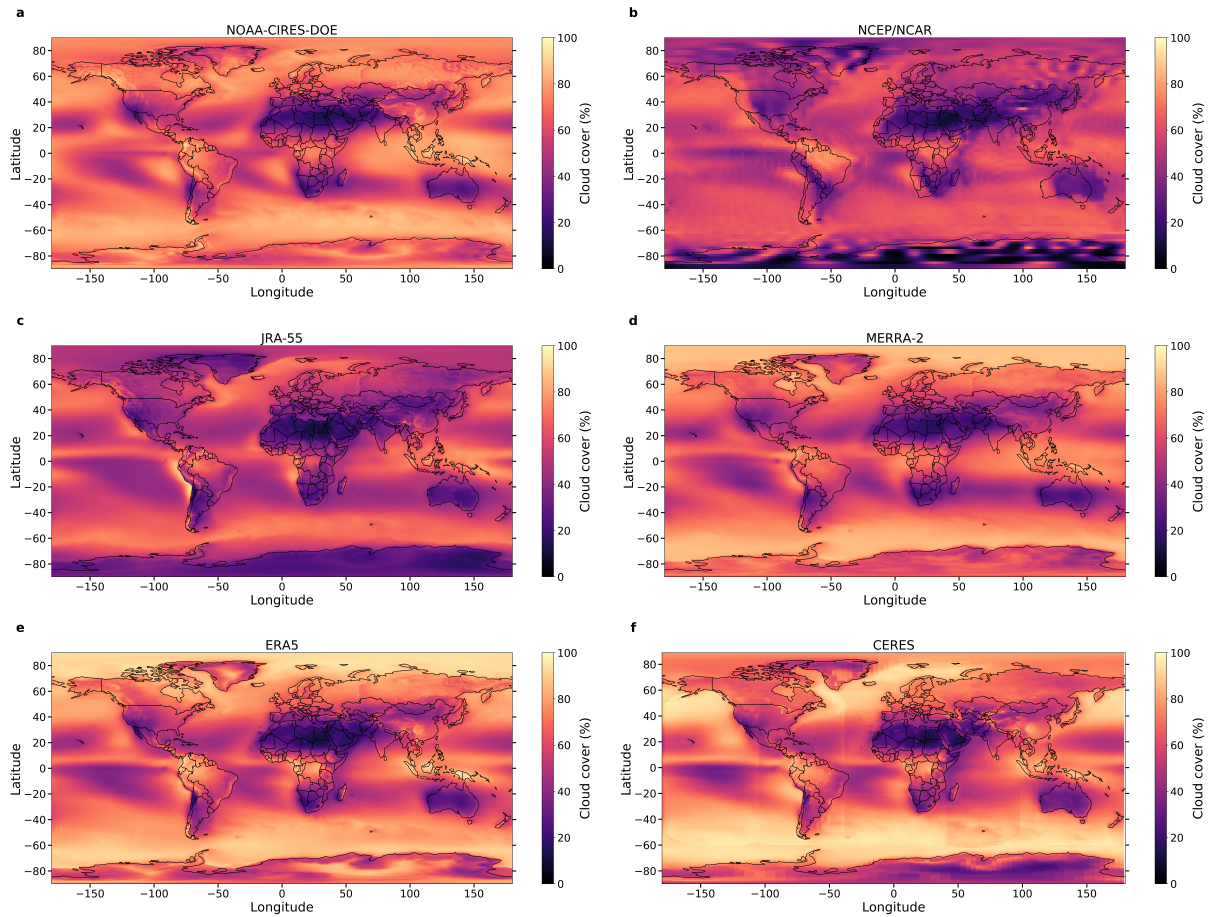
Fig. S5. Spatial distribution of cloud cover in **a** NOAA-CIRES, **b** NCEP/NCAR, **c** JRA-55, **d** MERRA-2, **e** ERA5, and **f** CERES for Common Period I (2001-2015).
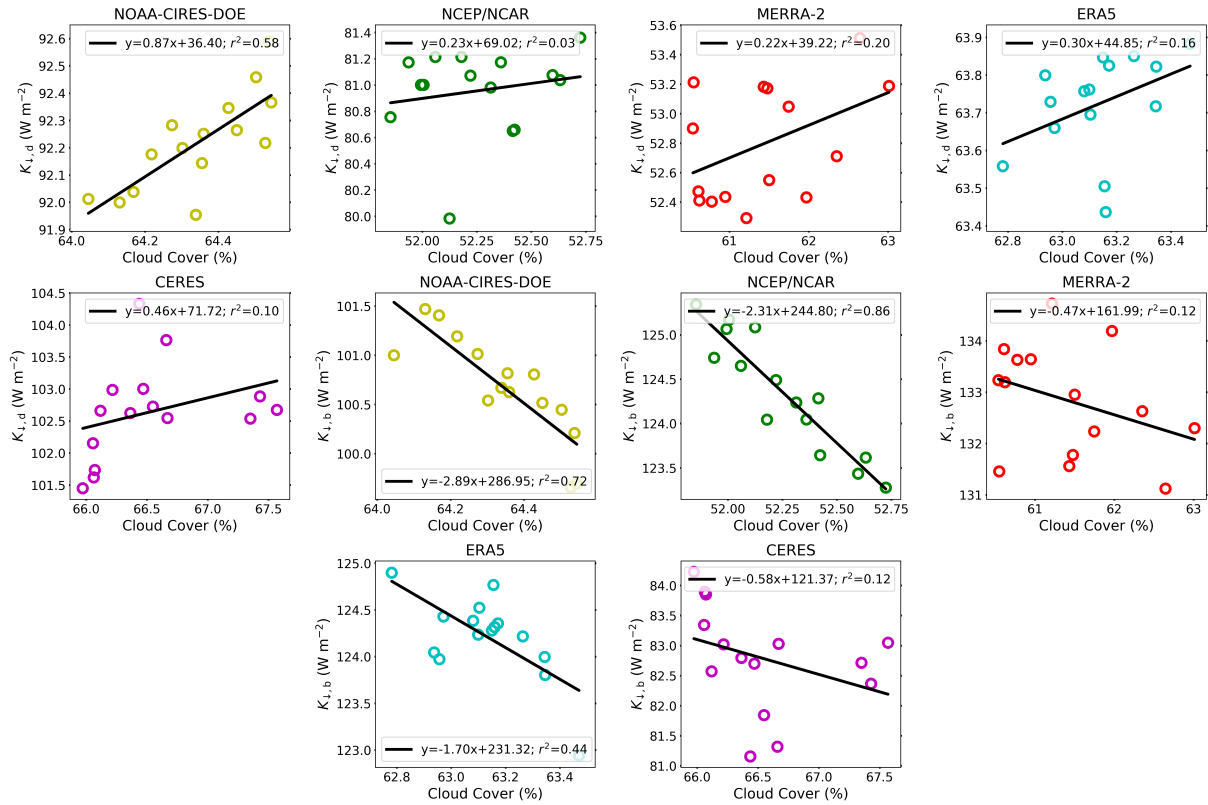
Fig. S6. Associations between annual average percentage cloud cover and surface radiation fields (incident diffuse radiation $K_{\downarrow,d}$ and direct beam radiation $K_{\downarrow,b}$) for Common Period I (2001-2015) for each of the gridded products. The lines of best fit and their equations are shown.